JOURNAL OF Applied Polymer SCIENCE

Structure, Thermal, and Mechanical Properties of DDM-Hardened Epoxy/Benzoxazine Hybrids: Effects of Epoxy Resin Functionality and ETBN Toughening

Sergiy Grishchuk,[1] Liubov Sorochynska,[1] Olof C. Vorster,[2] József Karger-Kocsis[2,3]

[1]Institut für Verbundwerkstoffe GmbH (Institute for Composite Materials), Kaiserslautern University of Technology, D-67663 Kaiserslautern, Germany

[2]Department of Polymer Technology, Faculty of Engineering and the Built Environment, Tshwane University of Technology, Pretoria 0001, Republic of South Africa

[3]Department of Polymer Engineering, Faculty of Mechanical Engineering, Budapest University of Technology and Economics, H-1111 Budapest, Hungary

Correspondence to: J. Karger-Kocsis (E-mail: karger@pt.bme.hu)

ABSTRACT: Bifunctional, trifunctional, and tetrafunctional epoxy (EP) resins were hardened with stoichiometric amount of 4,4'-diaminodiphenyl methane in presence and absence of benzoxazine (BOX). The EP/BOX ratio of the hybrid systems was constant, viz. 50/50 wt %. For the bifunctional EP, the EP/BOX range covered the ratios 75/25 and 25/75 wt %, as well. Epoxy-terminated liquid nitrile rubber (ETBN) was incorporated in 10 wt % in the systems with trifunctional and tetrafunctional EP, and in 10, 15, and 20 wt % in the EP/BOX with bifunctional EP to improve their toughness. Information on the structure and morphology of the hybrid systems was received from differential scanning calorimetric, dynamic-mechanical thermal analysis, atomic force microscopic, and scanning electron microscopic studies. The flexural, fracture mechanical properties, thermal degradation, and fire resistance of the EP/BOX and EP/BOX/ETBN hybrids were determined. It was found that some homopolymerized BOX was built in the EP/BOX conetwork in form of nanoscale inclusions, whereas ETBN formed micron scaled droplets of sea-island structure. Incorporation of BOX improved the charring and fire resistance, enhanced the flexural modulus and strength, reduced the glass transition (T_g), the fracture toughness, and energy. Additional modification with ETBN decreased the charring, fire resistance, flexural modulus and strength, as well as T_g, however, improved the fracture toughness and especially the fracture energy. © 2012 Wiley Periodicals, Inc. J. Appl. Polym. Sci. 000: 000–000, 2012

KEYWORDS: resins; thermosets; properties and characterization; crosslinking; flame retardance

Received 6 April 2012; accepted 31 May 2012; published online
DOI: 10.1002/app.38123

INTRODUCTION

Polybenzoxazines, formed by ring-opening polymerization of benzoxazine (BOX) precursors, are under spotlight of interest due to their excellent thermal properties (high glass transition temperature, T_g), low flammability (high char yield), high stiffness, low water uptake, and shrinkageless curing especially as matrix materials for composite applications.[1–3] Among the disadvantages of polybenzoxazines their high polymerization temperature (T > 200°C) and inherent brittleness have to be mentioned first. To find suitable catalysts, additives and modifications to reduce the polymerization temperature of BOX is still an active topic.[3,4] The necessity of toughness improvement was also early recognized and the related work mostly followed the strategy that was proven for epoxy (EP) based systems. This strategy is directed to manipulate the crosslinked structure via co-crosslinking, [2,4–9] and to incorporate or create a second, dispersed phase in the matrix.[1,3,4] Co-crosslinking of BOX with EP was always favored because the phenolic —OH groups of the ring-opened BOX could react with epoxy groups of EP, i.e., the role of the EP curing agent was overtaken by the BOX.[8,9] On the other hand, the fracture mechanical performance could not be markedly improved by the EP/BOX combinations. Therefore, the work on toughening focused on the use of preformed or *in situ* produced particles which are micro or nanoscaled. The *in situ* generated particles are from functionalized or nonfunctionalized rubbers and polymers, which are initially dissolved in the curable resin but segregates during their gelling/crosslinking. For EPs, the most powerful toughening agents are end-

Applied Polymer SCIENCE

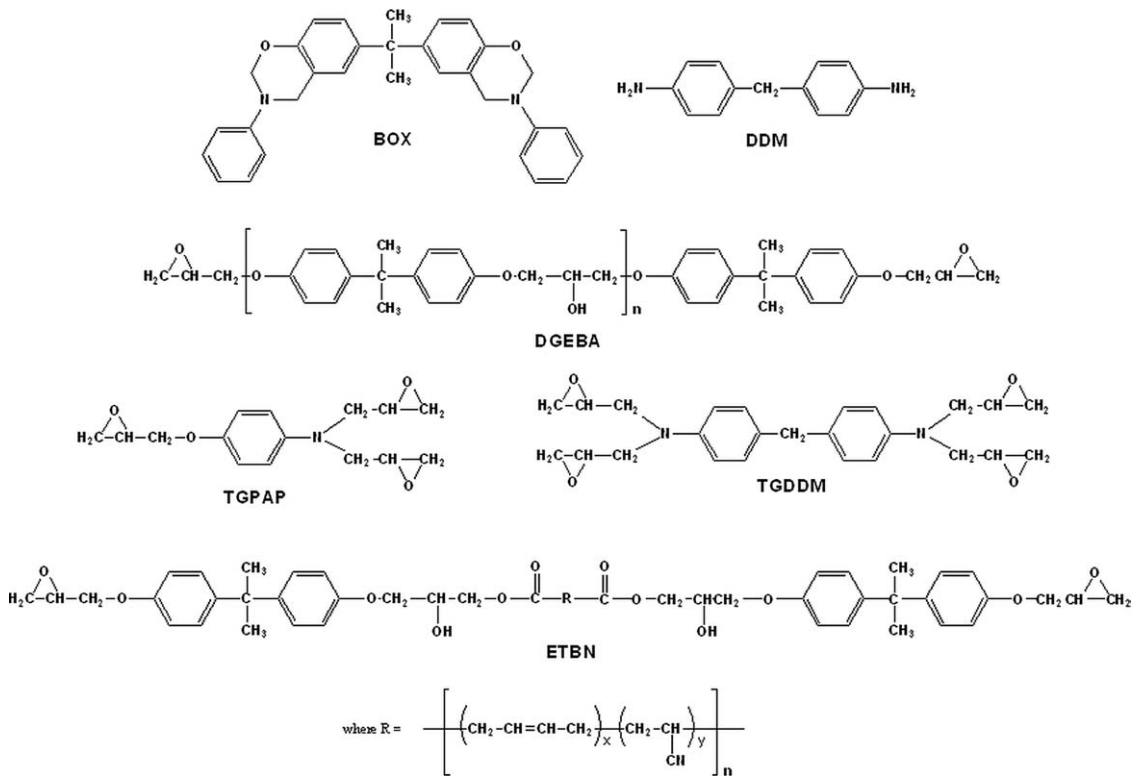

Figure 1. The chemical structures and abbreviations of the materials used.

functionalized liquid nitrile rubbers though their use is accompanied with penalties especially in stiffness and T_g. Amine- and carboxyl-terminated acrylonitrile-butadiene rubbers (ATBN and CTBN, respectively) have been tried in BOX and EP/BOX formulations already whereby the ATBN yielded better toughening than CTBN.[10–14] Lee et al.[15] used hydroxyl-terminated polybutadiene to enhance the toughness of polybenzoxazines. Core-shell type rubbers[14,16] and thermoplastic polymers (polyphenyleneoxide, polyethersulphone[14]), which are also well established toughener for EP resins,[17] were also investigated in BOX systems. It is noteworthy that works are in progress to create nanostructure by phase separation of multiblock copolymers containing BOX units which *per se* would yield enhanced toughness.[18]

In our recent works, we have investigated the structure-property relationships in (i) various amine-cured bifunctional EPs modified with a fixed amount of BOX,[19] and (ii) aromatic amine-cured bifunctional, trifunctional, and tetrafunctional EPs with varying amount of BOX.[20] The research interest was triggered by the fact that primary diamines, being usual hardeners for EPs, also react with BOX and accelerate the BOX homopolymerization at the same time.[19]

This work was aimed at rounding up this test series by checking whether epoxy-terminated liquid nitrile rubber (ETBN) is a suitable toughening agent for EP/BOX hybrids. Note that ETBN was not yet adapted for the toughening of BOX and BOX/EP systems. To get a deeper insight in the structure-property relationships, EPs with different functionalities were selected and cured with stoichiometric amount of aromatic diamine in absence and presence of BOX. The EP/BOX ratio was kept constant, namely 50/50 wt % except the bifunctional EP where this ratio covered 75/25 and 25/75 wt %, as well. ETBN was introduced in EP/BOX hybrids in 10 wt % amount except the bifunctional EP/BOX in which the ETBN content was set for 10, 15, and 20 wt %, respectively. The ETBN content selected is in that range which is usually recommended for EP toughening.

EXPERIMENTAL

Materials

The chemical structures of the materials used are depicted in Figure 1. The BOX used was an *N*-phenyl bisphenol A based 1,3-benzoxazine with a density of 1.18 g/mL at room temperature (RT), melting range of 80–85°C, and a dynamic viscosity range between 80 and 180 mPa·s at T = 125°C (Araldite MT 35,600 CH of Huntsman Advanced Materials, Basel, Switzerland). This BOX grade is usually abbreviated by Ba which, however, has been replaced by BOX throughout this article.

The bifunctional EP was a diglycidyl ether bisphenol A based grade, D.E.R. 331 from Dow Deutschland Anlagengesellschaft mbH (Schwalbach, Germany). This EP, further referred as DGEBA, had the following characteristics: epoxy equivalent weight (EEW): 182–192 g/eq., epoxide percentage: 22.4–23.6 %, dynamic viscosity, and density at T = 25°C 11–14 Pa·s and 1.16 g/mL, respectively. The trifunctional aromatic EP was triglycidyl *p*–aminophenol (further on TGPAP), produced under the trade name Araldite MY 0510 by Huntsman Advanced Materials. Its EEW was 95–106 g/eq., dynamic viscosity and density at T =

25°C 550–850 mPa·s and 1.21 g/mL, respectively. The tetrafunctional EP, Araldite MY 721, also from Huntsman Advanced Materials, was tetraglycidyl diaminodiphenylmethane (further on TGDDM) with the following characteristics: EEW 109–116 g/eq., dynamic viscosity at T = 50°C 3–6 Pa.s, and density at T = 25°C 1.21 g/mL. The dynamic viscosity data were determined in Ubbelohde capillary viscometer according to the ASTM D445 standard.

As EP hardener 4,4'-diaminodiphenyl methane (DDM) was chosen to guarantee a high glass transition temperature (T_g). DDM (melting temperature: 92°C) was procured from Sigma-Aldrich Chemie GmbH (Taufkirchen, Germany). It is noteworthy that DDM proved to be a weak accelerator of the BOX homopolymerization.[19]

The toughening agent was a styrene diluted (50 wt %) epoxy terminated liquid nitrile rubber, Hycar ETBN 1300 × 40 (further on ETBN) of Noveon (Brussels, Belgium). ETBN is an butadiene-acrylonitrile copolymer containing 17.5±2.0% acrylonitrile, Brookfield viscosity at 27°C of 1450±750 mPa·s, acid value of <1.5 mg (KOH)/g, and specific gravity at 25°C of 0.945. Actually, the polymeric portion of ETBN is a reaction product of 2 moles DGEBA and 1 mole of CTBN 1300 × 8 (carboxyl-terminated butadiene-acrylonitrile copolymer with acrylonitrile content of ∼ 17%, number-average molecular weight of 3550 g/mol, acid value of 29 mg (KOH)/g and functionality of 1.8 (0.052 equivalents per hundred rubber), being diluted with 50 wt % of styrene monomer.

Sample/Specimen Preparation

The samples were prepared as indicated below. First, the EP was warmed to 70°C and kept for 30 min to melt the eventually crystalline fraction. Next, the powdered BOX was added to the warm EP and mixed through (1900 revolutions per minute, rpm) for 5 min. The mix was placed in a thermostatic oven and kept at T = 120°C for 40 min to dissolve the BOX. After this step, the toughening agent was added and mixed at 200 rpm for 4 min. Hot ETBN containing mixtures were degassed *in vacuo* and stored at T = 120°C for additional 15 min. Afterward, the amine was introduced by mixing (160 rpm) for 4 min. Finally, the mixture was deareated *in vacuo* and poured in open molds manufactured from polytetrafluoroethylene (PTFE). The PTFE molds contained the cavities of the rectangular bars and compact tension (CT) specimens used for testing (see later).

The EP/amine ratio was stoichiometric in all recipes. Though the BOX reacts with both the amine compound and EP, it was considered as an inert material, i.e., the functionality of BOX has been disregarded. The EP (including hardener)/BOX ratio was kept constant, 50/50 wt %, for the systems studied, except DGEBA for which the EP/BOX ratio covered also 75/25 and 25/75 wt %. ETBN solution was added in 10 wt % in the EP/BOX = 50/50 wt % hybrids with EPs of various functionalities, as well as in DGEBA/BOX = 75/25 and 25/75 wt % systems. The ETBN content was varied (10, 15, and 20 wt %) for the DGEBA/BOX = 50/50 wt % hybrid.

The cure cycle (temperature vs. time) of the samples was disclosed in our earlier works.[19,20] The cure schedule composed of the following steps: 1 h (h) at T = 90°C, 4 h at T = 150°C, and 7 h at T = 180°C.

Morphology Determination

Morphology of the hybrid systems was studied by scanning electron and atomic force microscopy (SEM and AFM, respectively) techniques. The fracture surface of CT specimens (see later) was inspected in SEM using a JSM 5400 device of Jeol (Tokyo, Japan). The fracture surface was coated with an Au/Pd alloy prior to SEM inspection using a Balzers SCD 050 (Balzers, Lichtenstein) sputtering apparatus.

AFM scans were taken on polished samples by an AFM device (Veeco/Digital Instruments GmbH, Mannheim, Germany) in tapping mode, and the related height- and phase contrast images captured. Commercial silicon cantilever (Pointprobe®NCH of Nanosensors, Neuchatel, Switzerland) with a nominal tip radius of less than 10 nm (120 μm cantilever length, 4 μm thickness, 30 μm width, and spring constant at 42 Nm^{-1}, Nanosensors, Neuchatel, Switzerland) was used under its fundamental resonance frequency of about 330 kHz. The scan rates were set at 0.5 Hz for all images.

Thermal and Viscoelastic Properties

Differential scanning calorimetry (DSC 821e of Mettler Toledo, Giessen, Germany) was used to detect the T_g of the EP/BOX hybrids prepared. DSC thermograms were registered in the temperature range from T = 0°C to 300°C at a heating rate of 10°C/min under N_2 flushing (30 mL/min). The sample weight varied between 10 and 20 mg.

Dynamic-mechanical thermal analysis (DMTA) were taken on rectangular specimens (60 × 8 × 3 mm; length × width × thickness) in three point bending configuration (span length: 50 mm) at 1 Hz using a DMA Q800 of TA Instruments (New Castle, DE). Tests were performed at a constant amplitude (50 μm) using sinusoidal oscillation and under dynamic conditions in the interval from −100 to 300°C at a heating rate of 1°C/min.

Flexural and Fracture Mechanical Behavior

The flexural properties, namely, modulus and strength of the hybrid resins, were determined on rectangular specimens (60 × 8 × 3 mm; length × width × thickness) in three point bending at RT according to EN63. The span length of the specimens was 50 mm (similar to DMTA) and their loading on a Zwick 1474 (Zwick GmbH, Ulm, Germany) universal testing machine occurred with deformation rate v = 1 mm/min.

The fracture toughness (K_c) and fracture energy (G_c) were measured according to ISO 13,586-1 standard. The tests were done on the Zwick 1445 machine (Zwick GmbH, Ulm, Germany) at RT with a crosshead speed of v = 1 mm/min. The CT specimens (dimension: 35 × 35 × 3 mm; length × width × thickness) were notched before loading by sawing. The sawn notch of the CT specimens was sharpened by a razor blade. The razor blade, fixed in a rig, was positioned in the notch root before hitting the fixing rig with a hammer. This "taping" yielded the desired sharp crack.

Applied Polymer SCIENCE

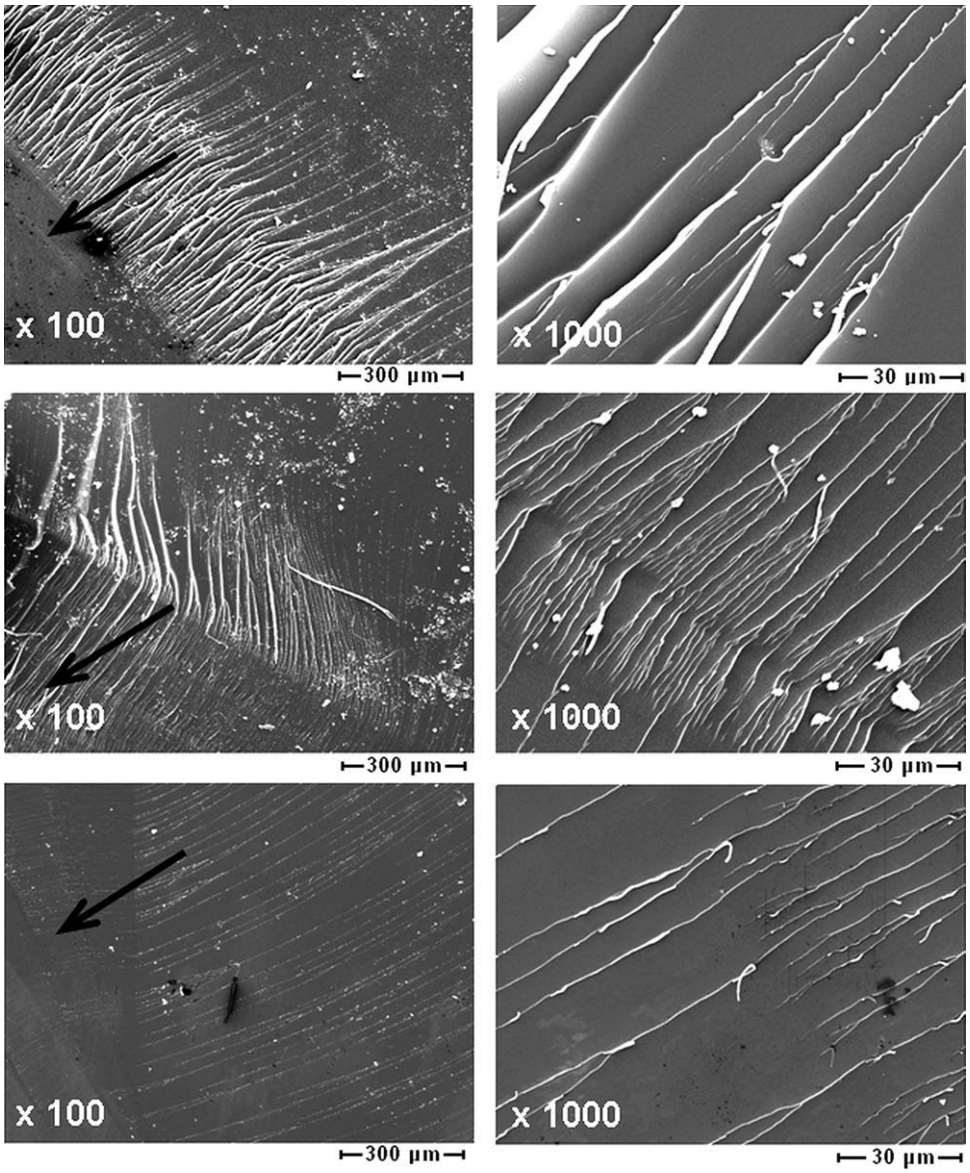

Figure 2. SEM pictures at different magnifications taken from the fracture surfaces of DGEBA/BOX (top), TGPAP/BOX (mid), and TGDDM/BOX (bottom) 50/50 wt % hybrids. Note: razor notching is indicated by arrow.

Thermogravimetric Analysis and Fire Resistance

The hybrid resins were subjected to thermogravimetric analysis (TGA) in a DTG-60 device of Shimadzu (Columbia, MD). The TGA experiments were conducted under nitrogen atmosphere (30 mL/min) in the temperature range from 25°C to 600°C with heating rate 10°C/min.

To test the fire resistance of the materials the UL 94V flammability vertical test was chosen being a stringent test. The materials were classified into burning groups (combustible, V0, V1, and V2) by considering the related criteria.[21]

RESULTS AND DISCUSSION

Morphology of the EP/BOX Hybrids

Figure 2 displays SEM pictures taken from the fracture surfaces of the bifunctional, trifunctional, and tetrafunctional EPs combined with BOX in 50/50 wt % ratio. For sake of brevity the fracture surfaces of the reference EPs are not shown being quite similar to those of the EP/BOX hybrids. Note that the roughness of the fracture surfaces of these hybrids decreases strongly with increasing EP functionality. Further, a well developed plastic zone can be resolved at the notch tip for DGEBA/BOX and TGPAP/BOX. Such a plastic zone is less perceptible in TGDDM/BOX. High magnification SEM pictures from this region display characteristic riverlike patterns. It is well accepted that the larger and the rougher the plastic zone the higher the fracture toughness and energy values are. This will be proved later. A further interesting aspect is that no separate BOX phase could be resolved in Figure 2. This means that either both EP and BOX are copolymerized, or the homopolymerized BOX is nanoscale dispersed in the EP matrix and therefore cannot be detected at low magnifications in SEM. The last assumption will be confirmed later by AFM results.

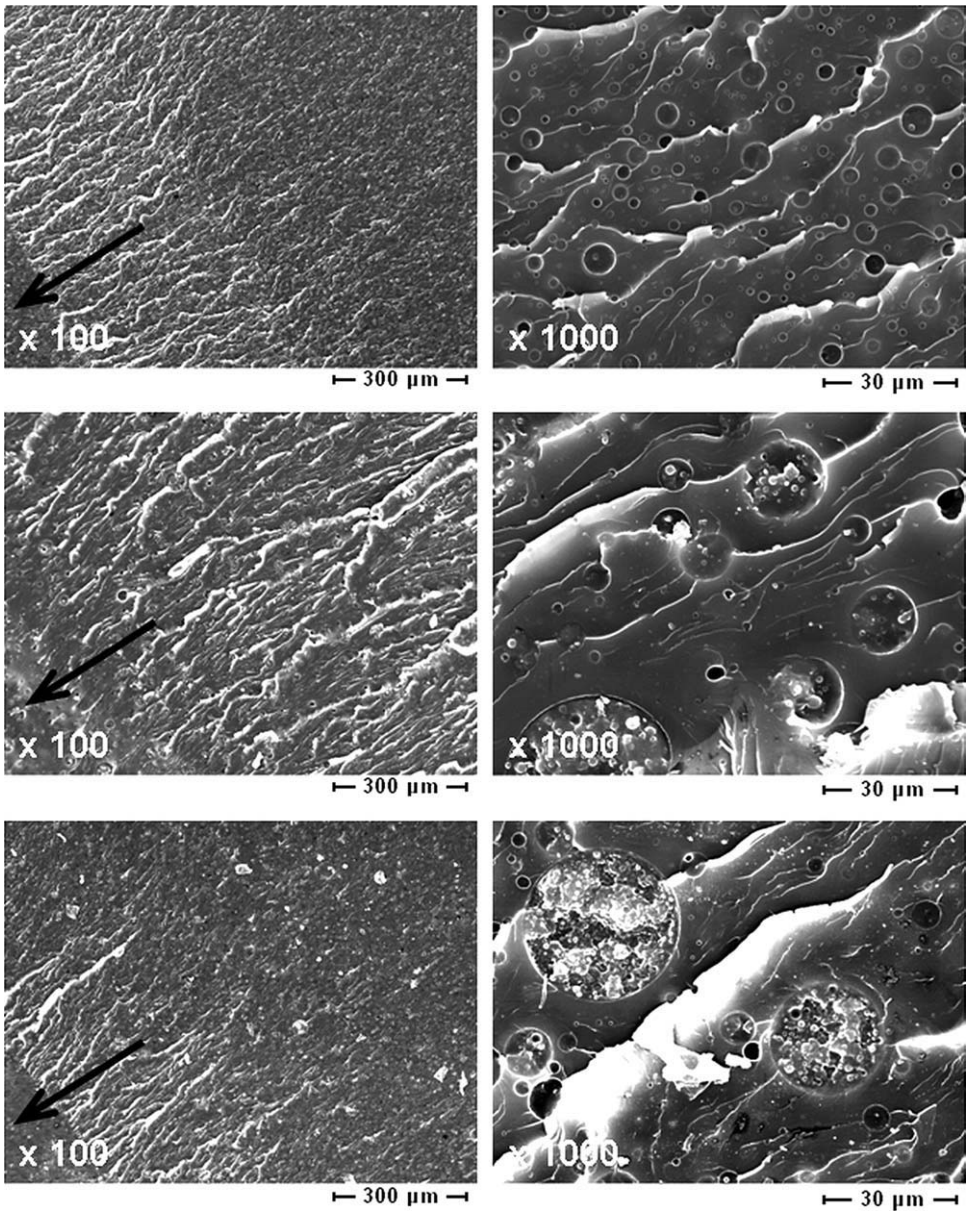

Figure 3. SEM pictures at different magnifications taken from the fracture surfaces of DGEBA/BOX (top), TGPAP/BOX (mid), and TGDDM/BOX (bottom) hybrids containing 10 wt % ETBN (EP/BOX/ETBN = 45/45/10 wt %). Note: razor notching is indicated by arrow; the plastic zone is clearly visible.

Incorporation of ETBN in 10 wt % contributes to the formation of a plastic zone (cf. Figure 3). This becomes especially clear when one compares the SEM pictures taken of TGDDM/BOX (cf. Figure 2) and TGDDM/BOX/ETBN (cf. Figure 3). The high magnification SEM pictures in Figure 3 also show that the coarse, microscaled ETBN particles should have contributed to toughness enhancement. This assumption is based on the fact that the particles are obviously cavitated and participated in crack pinning, as well. This facilitated the shear deformation of the EP ligaments between the particles which is the major energy absorbing mechanism.[17] It is worth of noting that the size of the ETBN particles becomes larger and their morphology more complex with increasing functionality of the EP. The ETBN particles exhibit a sea-island (also termed salami) structure because of the small EP inclusions within the large ETBN droplets. Recall that the ETBN contained styrene which could be thermally homopolymerized or copolymerized via the residual double bonds of the butadiene units of the ETBN rubber. Therefore, the small inclusions in the large ETBN droplets may also be of polystyrene nature. With increasing functionality of the EP the salami structure of the ETBN particles becomes more obvious (compare the right hand side SEM pictures in Figure 3). Parallel to that a better bonding between the ETBN particles and EP matrix can be observed. On the other hand, this sea-island morphology of ETBN becomes prominent also for the DGEBA/BOX = 50/50 wt % hybrids when the content

Applied Polymer SCIENCE

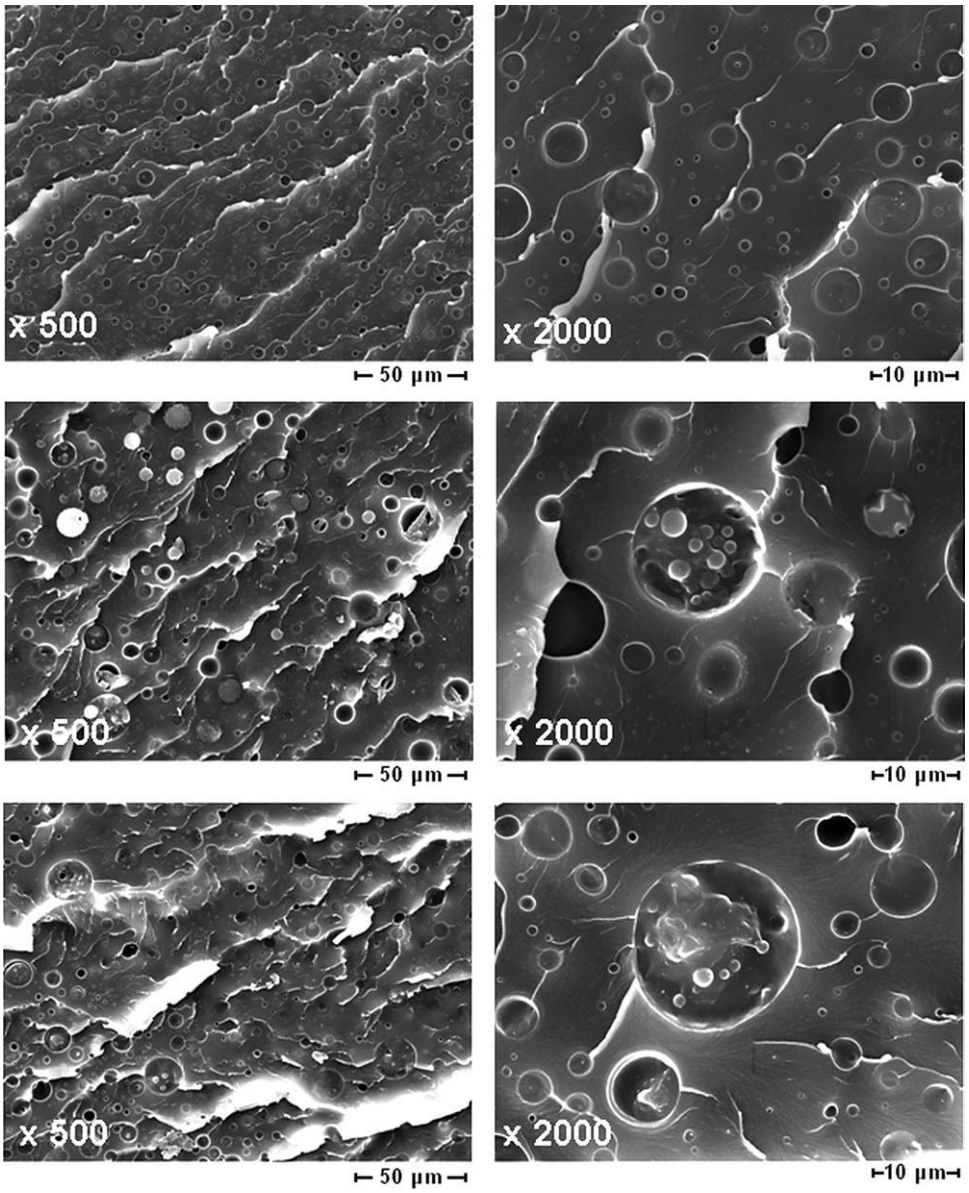

Figure 4. SEM pictures at different magnifications taken from the fracture surface of DGEBA/BOX/ETBN hybrids containing 10 (top), 15 (mid), and 20 (bottom) wt % of ETBN (DGEBA/BOX/ETBN = 45/45/10, 42.5/42.5/15, and 40/40/20 wt %, respectively).

of the ETBN rubber is higher than 10 wt % (cf. Figure 4). Figure 5 demonstrates on the example DGEBA/BOX = 75/25 wt % hybrid containing 10 wt % ETBN (DGEBA/BOX/ETBN = 67.5/22.5/10 wt %) that reduction of the BOX content also favors the sea-island structuring of the ETBN droplets. In the latter case, the ETBN particles are much better embedded in the EP matrix compared with systems containing higher amount of BOX (cf. SEM pictures in Figures 4 (top) and 5). So, ETBN particles with prominent sea-island morphology and good bonding to the matrix are formed when the hybrid composition is rich in multifunctional EP and ETBN. From the viewpoint of the morphology development it should be underlined that styrene is an efficient solvent for BOX, and ETBN itself is a coreactive modifier in our hybrid systems. It has to be underlined that final morphology of such multicomponent thermosets, as the present ones, is controlled by the cure kinetics affecting also the viscosity of the reaction mixture via the chemical reactions involved. In addition to the concurrent reactions disclosed for the EP/BOX/DDM system, the epoxy groups of ETBN may also react with the hydroxyls of the polymerized BOX and with the amine groups of the DDM. Further, via the double bonds both of ETBN and styrene (present as ETBN diluent) may undergo thermal induced radical polymerization.

To get a deeper insight into the EP/BOX matrix morphology the hybrids were subjected to AFM inspection. As example, the AFM height and phase contrast images, taken from the polished surfaces of the DGEBA/BOX = 50/50 wt % and DGEBA/BOX/ETBN = 45/45/10 wt % systems are displayed in Figures 6 and 7, respectively. The bright spots in the AFM phase images

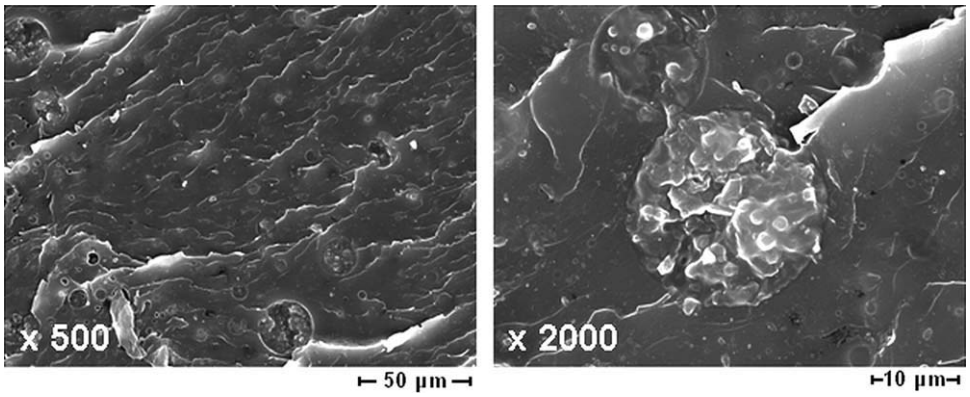

Figure 5. SEM pictures at different magnifications taken from the fracture surface of DGEBA/BOX/ETBN = 67.5/22.5/10 wt % hybrid.

represent the BOX. The latter is dispersed in coarse, partly merged domains in the EP matrix of the DGEBA/BOX hybrid. The size of BOX domains becomes more fine and its distribution more uniform in the hybrid containing 10 wt % ETBN (cf. Figure 7). This suggests that the final shape and size of inclusions is governed by the interplay between chemorheology and phase segregation kinetics. To check whether or not the BOX is fully polymerized, AFM work was done on polished specimens after etching in acetone for 35 min and follow-up drying in vacuum oven for 5 h (to recover the shape of the swollen EP matrix). Note that acetone should dissolve the unpolymerized BOX very quickly. Figure 8 shows that acetone etching did not change the morphology and thus the white inclusions in the AFM images represent the polymerized BOX, in fact. Small topological difference in the morphology of the initial and etched samples is due to etching/drying procedure applied. Further, it is hardly possible to scan exactly the same place on the sample surface after etching. However, one can recognize that acetone etching did not affect either the distribution or the average size of the nanoparticles which thus can be assigned to cured BOX. Nonetheless, further AFM studies on neat DDM-cured EP and unmodified crosslinked BOX are needed to support unequivocally the presence of nanoscale dispersed polymerized BOX in the hybrids. It is noteworthy that an AFM study on physically etched amine-cured EP yielded no evidence on a heterogeneous structure.[22]

Thermal and Viscoelastic Properties of EP/BOX Hybrids

The T_g values, read from the DSC scans, are listed in Table I. In all cases hybridization with BOX was associated with a shift in the T_g of the parent EPs toward lower temperatures. This shift in the T_g is caused by formation of an EP/BOX co-network which is different from that of the initial EP owing to coreactions of EP and DDM with BOX. A similar shift in T_g was found in our companion works.[19,20] The related T_g shift became more prominent with increasing functionality of the EP used (cf. Table I).

As expected, incorporation of ETBN and its increasing amount decreased the T_g values of the related systems. In addition, presence of ETBN reduced the BOX-related post-curing effect which was resolvable in the DSC scans at $T > 200$°C. This effect is probably due to the additional reaction of BOX (via the phenolic hydroxyl groups formed) with epoxy groups of the ETBN during curing.

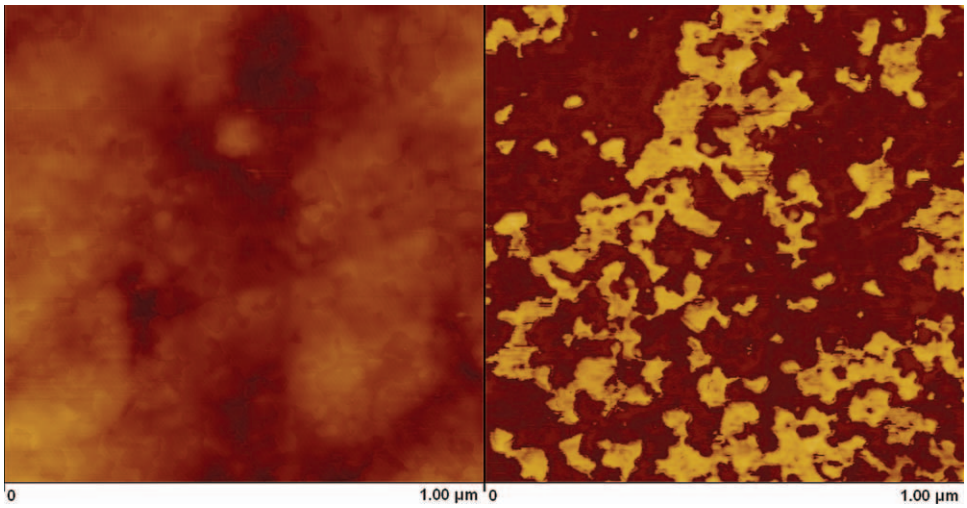

Figure 6. AFM height (left) and phase images (right) taken from the polished surface of DGEBA/BOX = 50/50 wt %. [Color figure can be viewed in the online issue, which is available at wileyonlinelibrary.com.]

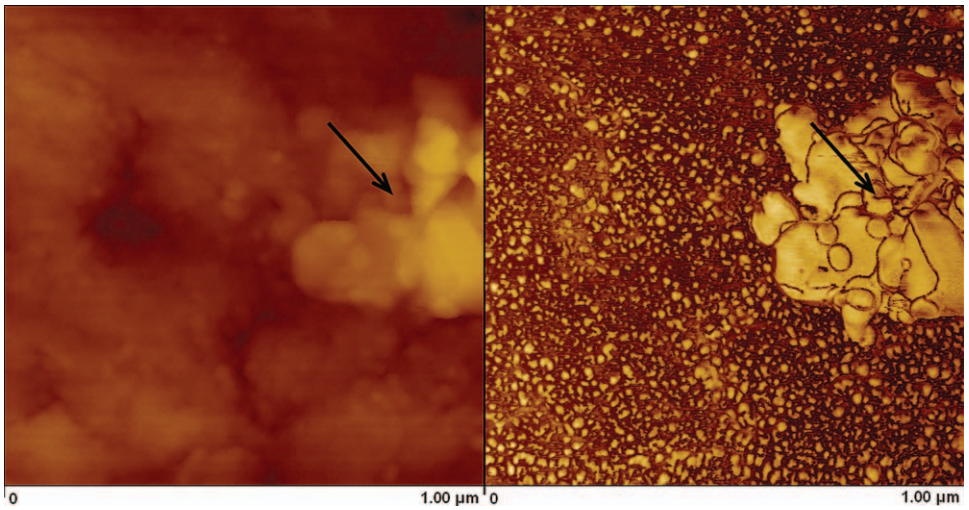

Figure 7. AFM height (left) and phase images (right) taken from the polished surface of DGEBA/BOX/ETBN = 45/45/10 wt %. Note: arrow indicate a part of a larger ETBN droplet. [Color figure can be viewed in the online issue, which is available at wileyonlinelibrary.com.]

The T_g data deduced from DSC tests have been confirmed by DMTA results. The temperature dependences of the storage modulus (E') and loss factor (tan δ) for the reference resins, EP/BOX = 50/50 wt %, and respective EP/BOX/ETBN systems are presented in Figure 9. Note that the DMTA traces of the reference EPs have already been published.[19,20] In general, one T_g was detected for all EP/BOX hybrids which reflects a high level of component compatibility. The T_g values, read as the peak

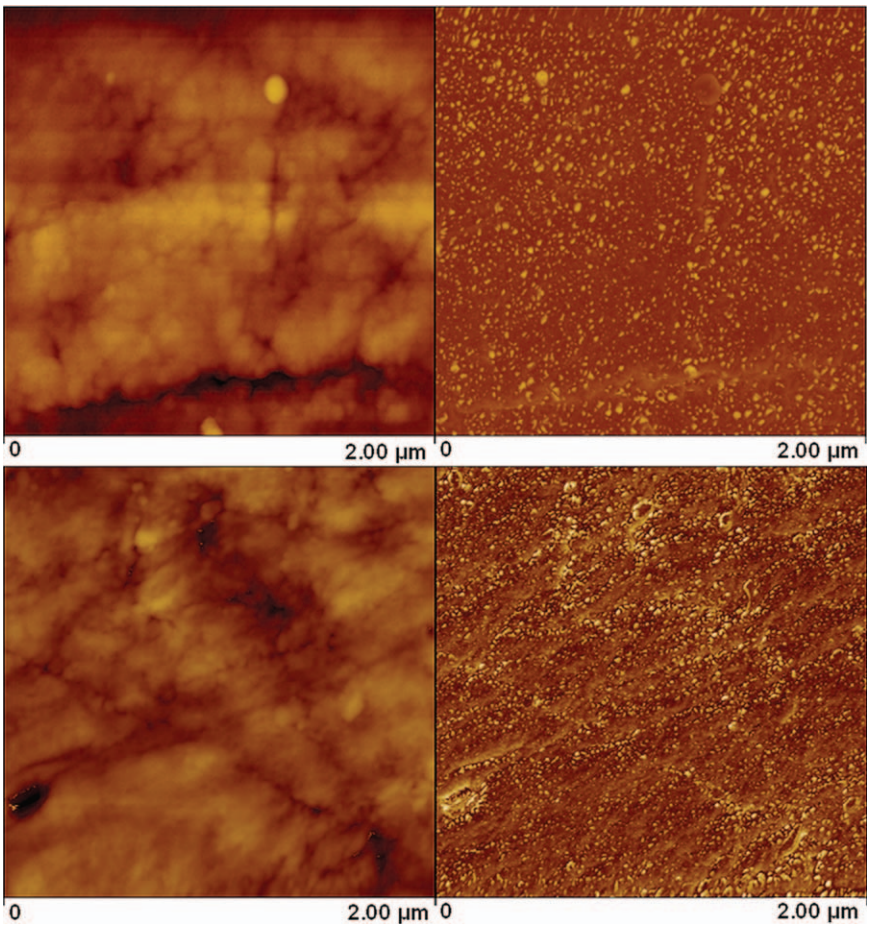

Figure 8. AFM height (left) and phase contrast (right) images taken from the polished surface of DGEBA/BOX/ETBN = 42.5/42.5/15 wt % hybrid before (top) and after acetone etching (bottom). [Color figure can be viewed in the online issue, which is available at wileyonlinelibrary.com.]

Table I. T_g, and Selected DMTA and TGA Data for the Resin Combinations Studied

System	T_g, °C		E', MPa		ν_c, mol/dm^3	$T_{2\%}$, °C	Char yield at T = 600°C, wt %
	DSC	DMTA	RT	T_g+30°C			
DGEBA-Ref	170	174	2627	43	3.61	365	18
DGEBA/BOX = 75/25	160	164	3725	30	2.58	342	22
DGEBA/BOX/ETBN = 67.5/22.5/10	157	159	2764	19	1.67	346	22
DGEBA/BOX = 50/50	162	173	4200	30	2.53	332	27
DGEBA/BOX/ETBN = 45/45/10	145	157	3251	16	1.39	332	28
DGEBA/BOX/ETBN = 42.5/42.5/15	132	150	3371	15	1.33	336	22
DGEBA/BOX/ETBN = 40/40/20	129	147	3098	14	1.25	330	23
DGEBA/BOX = 25/75	165	183	4405	30	2.47	319	30
DGEBA/BOX/ETBN = 22.5/67.5/10	156	173	4024	24	2.02	332	28
TGPAP-Ref	>210[a]	240	3841	84	6.20	308	27
TGPAP/BOX = 50/50	175	191	4436	55	4.46	311	28
TGPAP/BOX/ETBN = 45/45/10	163	185	4000	38	3.12	326	27
TGDDM-Ref	>210[a]	253	3680	59	4.25	312	26
TGDDM/BOX = 50/50	196	206	4508	59	4.65	319	25
TGDDM/BOX/ETBN = 45/45/10	178	189	3260	45	3.67	322	28
BOX-Ref	180	190	4976	41[b]	3.33	328	31

[a]Difficult to recognize exact because of strong overlapping with the postcuring exothermic peak, Postcuring disregarded.

temperatures of the α-relaxation transition in the tan δ vs. T traces, are also listed in Table I. The broad double-peak character of the α-relaxation should be noted for the reference polybenzoxazine (BOX-Ref) – cf. Figure 9(a). Very broad relaxation region indicates the broad size distribution of the relaxing segments being typical for irregular networks. Note that the second peak is related to postcuring effects. This is confirmed by increasing E'-values in the respective temperature interval (which cannot be resolved, however, in Figure 9(a) due to the linear scaling of E').

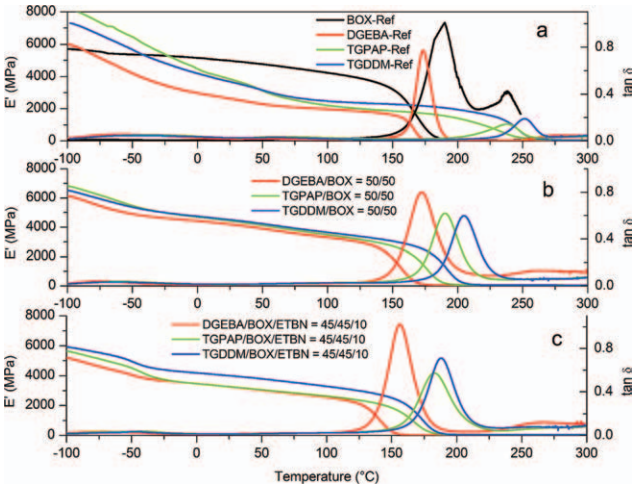

Figure 9. Storage modulus (E') and mechanical loss factor (tan δ) as a function of temperature and EP functionality for the reference resins (a), EP/BOX = 50/50 wt % (b) and EP/BOX/ETBN = 45/45/10 wt % hybrids (c). [Color figure can be viewed in the online issue, which is available at wileyonlinelibrary.com.]

The cocuring of EP with BOX is well reflected by the data of the rubber plateau modulus (E'_R). E'_R data were read at T_g+30°C for the EP and EP/BOX hybrids studied, and are also listed in Table I. The E'_R data were used to estimate the crosslink density according the theory of rubber elasticity:

$$\nu_c = E'_R/(3RT) \quad (1)$$

where ν_c is the crosslink density, R is the gas constant, and T is the absolute temperature. Usually the plateau modulus of crosslinked polymers is read at the temperature of T_g+30°C. It is the right place to mention that many groups working with BOX systems prefer to estimate the crosslink density through the Nielsen-equation[23] which is an alternative for the above mentioned one.

The influence of BOX on the DMTA behavior of the related hybrids showed some differences for the bifunctional and multifunctional epoxy resins. See that with increasing EP functionality both stiffness and T_g of the EP/BOX hybrids increase. The E' vs. T traces of DGEBA/BOX show that the homopolymerized BOX works as an efficient reinforcing phase [cf. Figure 9(a,b)]. The values of the storage modulus at RT, summarized in Table I, underline the BOX-induced antiplasticizing effect. Antiplastification means a stiffness increase parallel to T_g decrease.

The effect of ETBN incorporation on the DMTA response of the EP/BOX = 50/50 wt % hybrids is shown in Figure 9(c). Incorporation of ETBN in 10 wt % strongly reduces the stiffness and the T_g [cf. Figure 9(b,c)], which is characteristic for

plasticizers. Such stiffness reduction is typical for functionalized liquid rubber toughened EP systems. The step-like reduction in the stiffness of the EP/BOX/ETBN systems at T ~ –50°C is linked with the T_g of the ETBN. With increasing ETBN content the stiffness and T_g decrease as displayed by the DGEBA/BOX = 50/50 wt % hybrid (cf. Table I).

To sum up, the results obtained for EP/BOX hybrids are very characteristic for the antiplasticized systems. To find satisfactory explanation for the DMTA behavior of the hybrids, the secondary, and sub-T_g relaxation processes should be considered in details whereby special attention should be paid to the β-relaxation process of the EP and γ–relaxation of the polymerized BOX.

The β-transition corresponds to relaxation (motions) of small atomic groups, moieties, and their associates, which are much smaller than chain segments. According to the literature, the β-relaxation of EPs (at T ~ –60°C) is associated with crankshaft rotation of the hydroxyl ether structural units (—CH_2—CH(OH)—CH_2—O—), which is often overlapped with β-relaxation of aromatic groups (for example, diphenylpropane groups in case of DGEBA at T ~ –30°C) and is usually accompanied with an additional intermediate relaxation in the region between β- and α-relaxation transitions.[24]

It is clearly to see that structure and functionality of the parent EPs affect the β- and sub-T_g (intermediate) relaxations: (i) aminophenol based EP (TGPAP) has the highest temperature of the β-relaxation (about –30°C) and the highest intensity of sub-T_g relaxation transition: (ii) bisphenol A based EP (DGEBA) is characterized by the lowest β-transition temperature (ca. –60°C). Moreover, it has the highest intensity of the β- and the smallest intensity of the sub-T_g relaxation among the EPs; (iii) DDM based EP (TGDDM) showed some similarity to both other EPs (β-peak at ca. –50°C with the lowest intensity and sub-T_g transition with intermediate intensity).

Polymerized bisphenol A based BOX displays two sub-T_g relaxations: γ-relaxation in the region of T ca. –80 to –60°C (typical for bifunctional BOX resins) and a broad β-relaxation at about 80°C – cf. Figure 10(a). The latter transition is usually found in the temperature range of 10–100°C for bifunctional benzoxazines.[25–29] The submotion of pendant groups on the Mannich bridges (attached to the nitrogen atoms) and movements within them were also made responsible for the above mentioned low- and mid-temperature relaxation processes, respectively.[26] The β-relaxation peak of the neat EPs shifted toward lower temperatures and become narrower and less intense when hybridized with BOX [Figure 10(b)]. Hybridization with BOX was accompanied with a shift of the intermediate relaxation in sub-T_g region toward higher temperatures and with the onset of α-transition at lower temperatures (cf. Figure 10(a,b)].

In general, internal antiplasticization of EPs affects their viscoelastic properties via lowering their crosslinking density through deviation from the stoichiometry.[30] Increasing in storage modulus in the region between β- and α-transitions, lower T_g, lower storage modulus above the glass transition, and reduced intensity of the β-relaxation process compared with the reference system are characteristic features. The DMTA analysis revealed that the modification with BOX enhanced the stiffness (E-modulus),

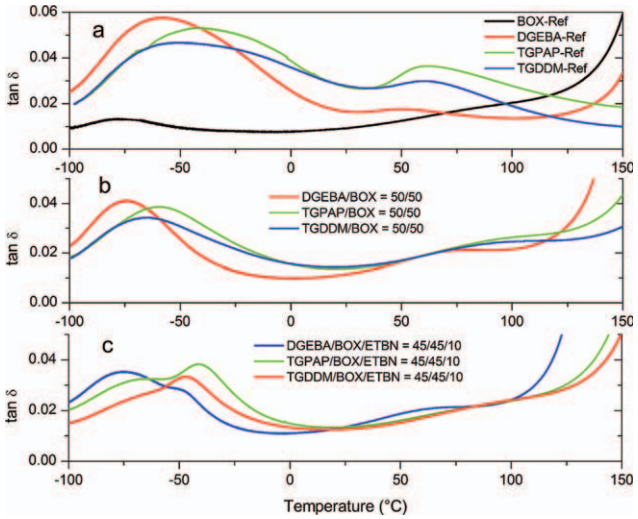

Figure 10. Mechanical loss factor (tan δ) as a function of temperature for the reference EPs and (a), EP/BOX = 50/50 wt % (b) and EP/BOX = 50/50 hybrids containing 10 wt % ETBN (EP/BOX/ETBN = 45/45/10 wt %) (c). [Color figure can be viewed in the online issue, which is available at wileyonlinelibrary.com.]

decreased the crosslink density and reduced the T_g (cf. Table I). The decreasing crosslink density of the hybrids can be traced to the low crosslinking density of the homopolymerized BOX and to the off-stoichiometry between EP and DDM. Note that the latter was caused by the reactions between the primary amine and BOX, and EP and BOX, respectively.[19,20]

Static Flexure and Fracture Mechanical Properties

The static flexural properties, i.e., E-modulus (E_f), strength (σ_f), and displacement at maximum load (ε_f) are listed in Table II. One can establish that E_f and σ_f increased, whereas the displacement at maximum load decreased with increasing BOX content for DGEBA/BOX. The same trend holds for the TGPAP and TGDDM networks when hybridized with BOX. This confirms that BOX acted as reinforcement in the related EP/BOX hybrids. ETBN yielded an adverse trend in the above properties. Higher E_f and the lower σ_f and ε_f values were found for BOX-Ref compared with those of reference EPs and EP/BOX systems.

The fracture mechanical data are also listed in Table II. Modification of DGEBA with BOX reduced both the fracture toughness (K_c) and fracture energy (G_c). On the other hand, practically no change in these fracture mechanical parameters could be noticed for the TGPAP/BOX and TGDDM/BOX systems. The possible reason behind this fact is that the fracture mechanical data of BOX-Ref do not differ practically from those of the TGPAP- and TGDDM-Ref. ETBN fulfilled its role as toughening agent. Its incorporation enhanced both K_c and G_c, and especially the fracture energy was prominently improved (cf. Table II). The fracture mechanical parameters DGEBA/BOX/ETBN hybrids were markedly enhanced with increasing ETBN content. Recall that with increasing ETBN content also the size distribution and morphology of the ETBN domains changed. The former became broader while the latter altered from a featureless to a sea-island type (cf. Figure 5). A similar trend can be observed for the TGPAP- and TGDDM-based hybrids when

Table II. Flexural and Fracture Mechanical Data for the EPs, BOX, and EP/BOX Hybrids

	Properties				
	Flexure			Fracture mechanics	
System	E_f [MPa]	σ_f [MPa]	ε_f [%]	K_c [MPa·m$^{1/2}$]	G_c [J·m^2]
DGEBA-Ref	2423 ± 257	122 ± 9	8.41 ± 0.82	0.80 ± 0.07	362 ± 54
DGEBA/BOX = 75/25	3250 ± 221	148 ± 15	6.41 ± 0.38	0.64 ± 0.08	214 ± 42
DGEBA/BOX = 50/50	3630 ± 108	147 ± 11	4.43 ± 0.58	0.69 ± 0.04	213 ± 21
DGEBA/BOX = 25/75	4655 ± 240	172 ± 19	3.75 ± 0.38	0.68 ± 0.03	210 ± 47
DGEBA/BOX/ETBN = 45/45/10	3183 ± 248	144 ± 16	4.74 ± 0.93	0.87 ± 0.06	384 ± 44
DGEBA/BOX/ETBN = 42.5/42.5/15	3176 ± 132	118 ± 11	3.77 ± 0.37	0.97 ± 0.03	417 ± 51
DGEBA/BOX/ETBN = 40/40/20	3160 ± 105	127 ± 14	4.50 ± 0.52	0.92 ± 0.02	470 ± 36
TGPAP-Ref	3498 ± 151	136 ± 13	5.37 ± 0.99	0.64 ± 0.04	162 ± 22
TGPAP/BOX = 50/50	4225 ± 318	144 ± 25	3.47 ± 0.76	0.63 ± 0.03	145 ± 28
TGPAP/BOX/ETBN = 45/45/10	2951 ± 345	80 ± 10	2.54 ± 0.66	0.60 ± 0.04	201 ± 15
TGDDM-Ref	3078 ± 149	126 ± 17	4.75 ± 0.97	0.63 ± 0.02	187 ± 13
TGDDM/BOX = 50/50	4266 ± 126	185 ± 21	4.56 ± 0.85	0.61 ± 0.02	115 ± 8
TGDDM/BOX/ETBN = 45/45/10	3654 ± 237	121 ± 24	3.26 ± 0.98	0.66 ± 0.13	295 ± 74
BOX-Ref	4597 ± 91	94 ± 28	1.86 ± 0.56	0.71 ± 0.04	176 ± 24

modified with ETBN (cf. Figure 4). On the other hand, no general information can be deduced whether sea-island structured domains result in higher toughening than those without in our systems.

TGA and Fire Resistance

The TGA data found for the DGEBA and DGEBA/BOX systems confirm that BOX incorporation improved the charring – cf. Table I. This was, however, not the case with TGPAP and TGDDM. Obviously, their thermal degradation behavior is controlled by the EP itself. The temperature values linked with 2 wt % loss ($T_{2\%}$), and the char yield at T = 600°C are listed for all hybrids in Table I. Surprisingly the incorporation of ETBN did not reduce considerably either the $T_{2\%}$ or the char values. This may be traced to the complex morphology of the ETBN particles which are chemically bonded to the matrix.

Table III. . UL-94V Flame Test Results for the EPs, BOX and EP/BOX Hybrids

	First ignition		Second ignition		
System	Average burning time, s	Dripping	Average burning time, s	Dripping	UL-94 classification
DGEBA-Ref	51	No	10	no	Combustible
DGEBA/BOX = 75/25	24	No	9	no	V-1
DGEBA/BOX = 50/50	28	No	3	no	V-1
DGEBA/BOX = 25/75	23	No	2	no	V-1
DGEBA/BOX/ETBN = 67.5/22.5/10	28	No	10	no	V-1
DGEBA/BOX/ETBN = 45/45/10	23	No	11	no	V-1
DGEBA/BOX/ETBN = 42.5/42.5/15	22	No	24	no	V-1
DGEBA/BOX/ETBN = 40/40/20	32	No	57	no	Combustible
DGEBA/BOX/ETBN = 22.5/67.5/10	23	No	11	no	V-1
TGPAP-Ref	57	Yes	8	no	Combustible
TGPAP/BOX = 50/50	30	No	11	no	Combustible
TGPAP/BOX/ETBN = 45/45/10	35	No	14	no	Combustible
TGDDM-Ref	48	yes	43	yes	Combustible
TGDDM/BOX = 50/50	23	no	7	no	V-1
TGDDM/BOX/ETBN = 45/45/10	54	yes	4	no	Combustible
BOX-Ref	19	no	2	no	V-1

Table III lists the results of the vertical flame resistance tests. One can see that hybridization with BOX generally improves the resistance to dripping and flame, as well. By contrast, toughening with ETBN causes an adverse tendency with respect to these characteristics.

CONCLUSION

Aromatic amine (DDM) curable EP resins of different functionalities were modified with BOX and ETBN. The morphology and various properties (thermal, thermomechanical, thermogravimetric, fire resistance, flexure and fracture mechanical) of the hybrids and corresponding EP reference materials were determined. Results of this work can be summarized as follows:

Network Structure and Morphology

Curing of amine hardener containing EP with BOX resulted in a co-network formation. This contained nanoscale inclusions of the homopolymerized BOX. The dispersion of the homopolymerized BOX changed with the type/functionality of EP and ETBN modification. ETBN was micron scaled dispersed and the related droplets exhibited pronounced sea-island structure. The morphology of the ETBN droplets became more complex with increasing ETBN and EP amounts, and EP functionality in the corresponding hybrids.

Mechanical Properties

BOX incorporation enhanced the stiffness (E-modulus) and strength based on DMTA and flexural tests, whereas ETBN resulted in an adverse trend. This was explained by the antiplasticizing and plasticizing effects of the nanoscale homopolymerized BOX and microscale ETBN droplets, respectively. Hybridization of EP with BOX reduced the fracture toughness and energy compared with the EP references. Additional incorporation of ETBN improved these fracture mechanical parameters, as expected. Toughness enhancement was achieved by the ETBN droplets which cavitated, triggered crack pinning, and induced shear yielding of the EP matrix ligaments in between of the ETBN particles.

Thermal and Fire Resistance Properties

The T_g of the EP/BOX hybrids was lower than the reference EP that was traced to off-stoichiometry caused by the amine/oxazine and EP/BOX reactions. The effect of BOX on the char yield diminished with increasing EP functionality. Surprisingly, ETBN incorporation slightly improved the resistance to thermal degradation and charring but reduced the flame retardancy, especially with its increasing amount.

ACKNOWLEDGMENTS

This work was done in the framework of a collaboration project between Germany and South Africa, supported by BMBF and NRF, respectively, and also connected to the grant NK 83421given by the Hungarian Scientific Research Fund (OTKA). The authors are thankful to Mr. S. Schmitt and Mr. J. Mersch (Institute for Composite Materials, Kaiserslautern University of Technology) for the AFM investigations.

REFERENCES

1. Reghunadhan Nair, C. P. *Prog. Polym. Sci.* **2004,** *29*, 401.
2. Yagci, Y.; Kiskan, B.; Ghosh, N. N. *J. Polym. Sci. Polym. Chem.* **2009,** *47*, 5565.
3. Kiskan, B.; Ghosh, N. N.; Yagci, Y. *Polym. Int.* **2011,** *60*, 167.
4. Chernykh, A.; Agag, T.; Ishida, H. *Polymer* **2009,** *50*, 3153.
5. Lin, H. T.; Lin, C. H.; Hu, Y. M.; Su, W. C. *Polymer* **2009,** *50*, 5685.
6. Kimura, H.; Ohtsuka, K.; Matsumoto, A. *Exp. Polym. Lett.* **2011,** *5*, 1113.
7. Jubsilp, C.; Takeichi, T.; Rimdusit, S. *Polym. Degrad. Stab.* **2011,** *96*, 1047.
8. Ishida, H.; Allen, D. J. *Polymer* **1996,** *37*, 4487.
9. Kimura, H.; Matsumoto, A.; Ohtsuka, K. *J. Appl. Polym. Sci.* **2009,** *112*, 1762.
10. Jang, J.; Seo, D. *J. Appl. Polym. Sci.* **1998,** *67*, 1.
11. Jang, J.; Yang, H. *Compos. Sci. Technol.* **2000,** *60*, 457.
12. Agag, T.; Takeichi, T. *High Perform. Polym.* **2001,** *13*, S327.
13. Takeichi, T.; Agag, T. *High Perform. Polym.* **2006,** *18*, 777.
14. Gietl, T.; Lengsfeld, H.; Altstädt, V. *J. Mater. Sci.* **2006,** *41*, 8226.
15. Lee, Y. -. H.; Allen, D. J.; Ishida, H. *J. Appl. Polym. Sci.* **2006,** *100*, 2443.
16. Yang, L. Q.; Zhang, C.; Pilla, S.; Gong, S. *Compos. A* **2008,** *39*, 1653.
17. Grishchuk, S.; Gryshchuk, O.; Weber, M.; Karger-Kocsis, J. *J. Appl. Polym. Sci.* **2012,** *123*, 1193.
18. Li, Y.; Zheng, S. *J. Polym. Sci. Part. B: Pol. Phys.* **2010,** *48*, 1148.
19. Grishchuk, S.; Mbhele, Z.; Schmitt, S.; Karger-Kocsis, J. *Expr Polym. Lett.* **2011,** *5*, 273.
20. Grishchuk, S.; Schmitt, S.; Vorster, O. C.; Karger-Kocsis, J. *J. Appl. Polym. Sci.* **2012,** *124*, 2824.
21. Troitzsch, J. In International Plastics Flammability Handbook; Hanser: Munich, **1990;** pp 347–348.
22. Karger-Kocsis, J.; Gryshchuk, O.; Schmitt, S. *J. Mater. Sci.* **2003,** *38*, 413.
23. Nielsen, L. E.; Landel, R. F. In Mechanical Properties of Polymers and Composites; Marcel Dekker: New York, **1994.**
24. Kosmidou, T.hV.; Vatalis, A. S.; Delides, C. G.; Logakis, E.; Pissis, P.; Papanicolaou, G. C. *Expr. Polym. Lett.* **2008,** *2*, 364.
25. Rimdusit, S.; Ishida, H. *J. Pol. Sci. Phys.* **2000,** *38*, 1687.
26. Allen, D. J.; Ishida, H. *J. Appl. Polym. Sci.* **2006,** *101*, 2798.
27. Wang, Y.-X; Ishida, H. *J. Appl. Polym. Sci.* **2002,** *86*, 2953.
28. Wirasate, S.; Dhumrongvaraporn, S.; Allen, D. J.; Ishida, H. *J. Appl. Polym. Sci.* **1998,** *70*, 1299.
29. Ning, X.; Ishida, H. *J. Pol. Sci. Phys.* **1994,** *32*, 921.
30. Pascault, J.-P.; Sautereau, H.; Verdu, J.; Williams, R. J. J. In Thermosetting Polymers; Marcel Dekker: New York, **2002;** pp 334–336.